General and Comparative Endocrinology 277 (2019) 90–103

Contents lists available at ScienceDirect

General and Comparative Endocrinology

journal homepage: www.elsevier.com/locate/ygcen

Characterization of channel catfish (*Ictalurus punctatus*) melanocortin-3 receptor reveals a potential network in regulation of energy homeostasis

Li-Kun Yang[a], Zheng-Rui Zhang[a,b], Hai-Shen Wen[c], Ya-Xiong Tao[a,*]

[a] Department of Anatomy, Physiology and Pharmacology, College of Veterinary Medicine, Auburn University, Auburn, AL 36849, United States
[b] Key Laboratory of Marine Genetics and Breeding, Ministry of Education, College of Marine Life Sciences, Ocean University of China, Qingdao, China
[c] College of Fisheries, Ocean University of China, Qingdao, China

ARTICLE INFO

Keywords:
Channel catfish
Melanocortin-3 receptor
Melanocortin receptor accessory protein 2
Ligand binding
Signaling
Constitutive activity

ABSTRACT

The melanocortin-3 receptor (MC3R) is known to be involved in regulation of energy homeostasis, regulating feed efficiency and nutrient partitioning in mammals. Its physiological roles in non-mammalian vertebrates, especially economically important aquaculture species, are not well understood. Channel catfish (*Ictalurus punctatus*) is the main freshwater aquaculture species in North America. In this study, we characterized the channel catfish MC3R. The *mc3r* of channel catfish encoded a putative protein (ipMC3R) of 367 amino acids. We transfected HEK293T cells with ipMC3R plasmid for functional studies. Five agonists, including adrenocorticotropin, α-melanocyte stimulating hormone (α-MSH), β-MSH, [Nle^4, D-Phe^7]-α-MSH, and D-Trp^8-γ-MSH, were used in the pharmacological studies. Our results showed that ipMC3R bound β-MSH with higher affinity and D-Trp^8-γ-MSH with lower affinity compared with human MC3R. All agonists could stimulate ipMC3R and increase intracellular cAMP production with sub-nanomolar potencies. The extracellular signal-regulated kinases 1 and 2 (ERK1/2) activation could also be triggered by ipMC3R. The ipMC3R exhibited constitutive activities in both cAMP and ERK1/2 pathways, and Agouti-related protein served as an inverse agonist at ipMC3R, potently inhibiting the high basal cAMP level. Moreover, we showed that melanocortin receptor accessory protein 2 (MRAP2) preferentially modulated ipMC3R in cAMP production rather than ERK1/2 activation. Our study will assist further investigation of the physiological roles of the ipMC3R, especially in energy homeostasis, in channel catfish.

1. Introduction

The melanocortin receptors (MCRs), from melanocortin-1 to -5 receptors (MC1R to MC5R), are members of family A G protein-coupled receptors (GPCRs) that play significant roles in regulating diverse physiological processes, such as skin and hair pigmentation (MC1R) (Valverde et al., 1995), adrenal steroidogenesis (MC2R) (Mountjoy et al., 1992), energy homeostasis (MC3R and MC4R) (Cone, 2006), and exocrine gland secretion (MC5R) (Chen et al., 1997) (reviewed in (Cone, 2006; Tao, 2017).

MC3R and MC4R, with high expression in central nervous system, are also known as neural MCRs (Gantz et al., 1993a,b; Mountjoy et al., 1994; Roselli-Rehfuss et al., 1993). These two MCRs have been extensively studied in obesity pathogenesis due to their important functions in regulating energy homeostasis. Targeted deletion of either *Mc3r* or *Mc4r* in mice results in the obesity phenotype (Butler et al., 2000; Chen et al., 2000; Huszar et al., 1997). Human genetic studies also showed that mutations in *MC3R* or *MC4R* are associated with obesity (reviewed in (Demidowich et al., 2017; Hinney et al., 2013; Tao, 2009, 2010b; Yang and Tao, 2016b)). Although both MC3R and MC4R are important regulators of energy homeostasis, the mechanisms involved are distinct. MC4R primarily regulates food intake and energy expenditure (Balthasar et al., 2005; Tao, 2010a), whereas MC3R regulates feed efficiency (the ratio of weight gain to food intake) and nutrient partitioning (Butler et al., 2000; Chen et al., 2000; Zhang et al., 2005), maintaining circadian rhythm, and adapting to fasting (Begriche

Abbreviations: ACTH, adrenocorticotropin; AgRP, Agouti-related peptide; ERK1/2, extracellular signal-regulated kinases 1 and 2; Gi, inhibitory G protein; GPCR, G protein-coupled receptor; Gs, stimulatory G protein; hMC3R, human melanocortin-3 receptor; ipMC3R, *Ictalurus punctatus* melanocortin-3 receptor; ipMRAP2, *Ictalurus punctatus* melanocortin receptor accessory protein 2; MC3R, melanocortin-3 receptor; MCR, melanocortin receptor; MRAP, melanocortin receptor accessory protein; MSH, melanocyte-stimulating hormone; NDP-MSH, [Nle^4, D-Phe^7]-α-melanocyte stimulating hormone; POMC, proopiomelanocortin; RIA, radioimmunoassay; TMD, transmembrane domain

* Corresponding author.
E-mail address: taoyaxi@auburn.edu (Y.-X. Tao).

https://doi.org/10.1016/j.ygcen.2019.03.011
Received 9 December 2018; Received in revised form 12 March 2019; Accepted 18 March 2019
Available online 21 March 2019
0016-6480/

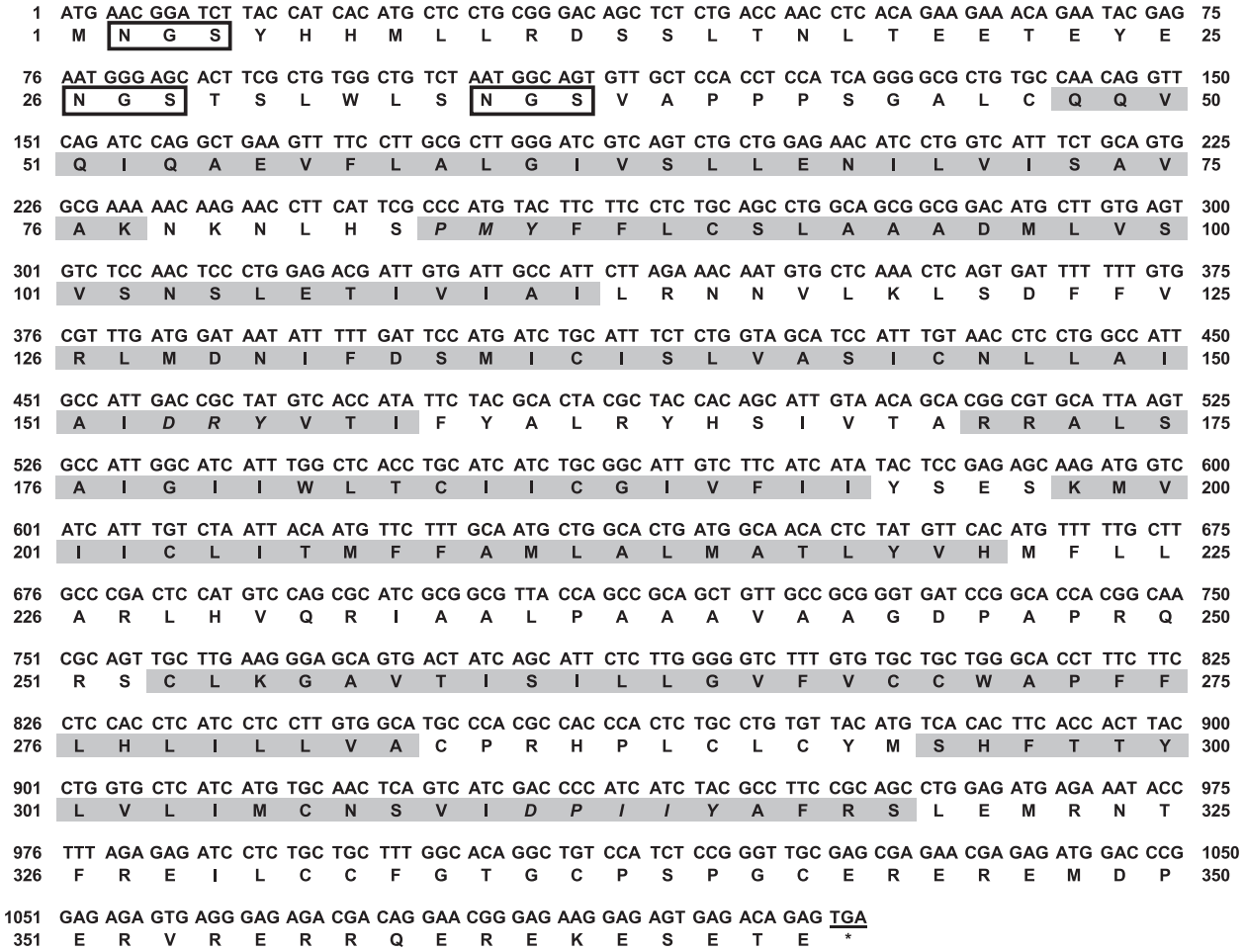

Fig. 1. Nucleotide and deduced amino acid sequence of ipMC3R. Positions of nucleotide and amino acid sequences are indicated on both sides. The seven TMDs are shaded in grey. The conserved motifs (PMY, DRY, and DPIIY) are highlighted in italic. Open boxes frame tripeptide sequences with the consensus sequence for *N*-linked glycosylation sites. Asterisk (*) denotes stop codon.

et al., 2012; Girardet and Butler, 2014; Sutton et al., 2010). *Mc3r* knockout mice display a moderate obesity phenotype with altered nutrient partitioning (increased fat mass and reduced lean mass) despite normal food intake or even hypophagia, which may be explained by subtle imbalance between fat intake and oxidation (Sutton et al., 2006). Recent studies also showed that *Mc3r* knockout mice exhibit reduced wakefulness before food presentation and abnormal rhythmic expression of clock genes (Girardet and Butler, 2014), as well as anomalous metabolic adaption to restricted feeding (Begriche et al., 2012). Cone and colleagues suggested that MC3R sets the upper and lower boundaries of energy homeostasis (Ghamari-Langroudi et al., 2018).

In addition to the central expression, MC3R has also been shown to be expressed in several peripheral tissues, indicating other potential physiological functions in the periphery. For example, the expression of MC3R can be detected in immune cells, such as macrophages, including both human and rodent macrophage cell lines and primary macrophages from different tissues (review in (Patel et al., 2011)). MC3R is an important modulator in immune response with effective anti-inflammatory and pro-resolving actions (Patel et al., 2011).

MC3R primarily couples to the heterotrimeric stimulatory G protein (Gs) to activate adenylyl cyclase, thereby increasing intracellular cAMP production and subsequent protein kinase A (PKA) activation. MC3R activation also triggers extracellular signal-regulated kinases 1 and 2 (ERK1/2) phosphorylation (Chai et al., 2007; Huang and Tao, 2014; Yang et al., 2015a,b; Yang and Tao, 2016a). The endogenous ligands for MC3R include four agonists (α-, β-, and γ-melanocyte-stimulating hormones (MSHs), and adrenocorticotropin (ACTH)) produced from post-translational processing of the precursor protein, proopiomelanocortin (POMC), and one antagonist, Agouti-related peptide (AgRP).

Recently, two small single transmembrane proteins, melanocortin receptor accessory proteins (MRAPs), including MRAP1 and MRAP2, have been shown to interact with and modulate MCR functions (Rouault et al., 2017). MRAP2, with its highly central expression, is more involved in regulation of energy homeostasis. Mice with *Mrap2* deletion display severe obesity (Asai et al., 2013; Novoselova et al., 2016). Potential pathogenic *MRAP2* mutations have also been identified in humans with early-onset obesity (Asai et al., 2013; Schonnop et al., 2016). MRAP2 modulation of MC4R signaling is an important pathway for regulating energy homeostasis in mammals and other species such as zebrafish and chicken (Sebag et al., 2013; Zhang et al., 2017). In addition, the role of MRAP2 on modulation of energy homeostasis through MC3R has also been suggested (Chan et al., 2009; Zhang et al., 2017). Therefore, MC3R and MC4R, together with α-MSH, AgRP, and MRAP2, form a complex system within the hypothalamus which connects the neural pathways governing satiety and metabolism with external signals of metabolic status to maintain energy homeostasis.

Although MC3R is well studied in humans and rodents, the functional studies of teleost MC3Rs are still very limited, potentially due to the absence of *mc3r* genes in some teleosts, such as fugu, medaka, and stickleback (Klovins et al., 2004a; Logan et al., 2003; Selz et al., 2007). Channel catfish (*Ictalurus punctatus*), belonging to the family of Ictaluridae, is the most extensively cultured species in North America. The genome and transcriptome data of this species have shown that channel

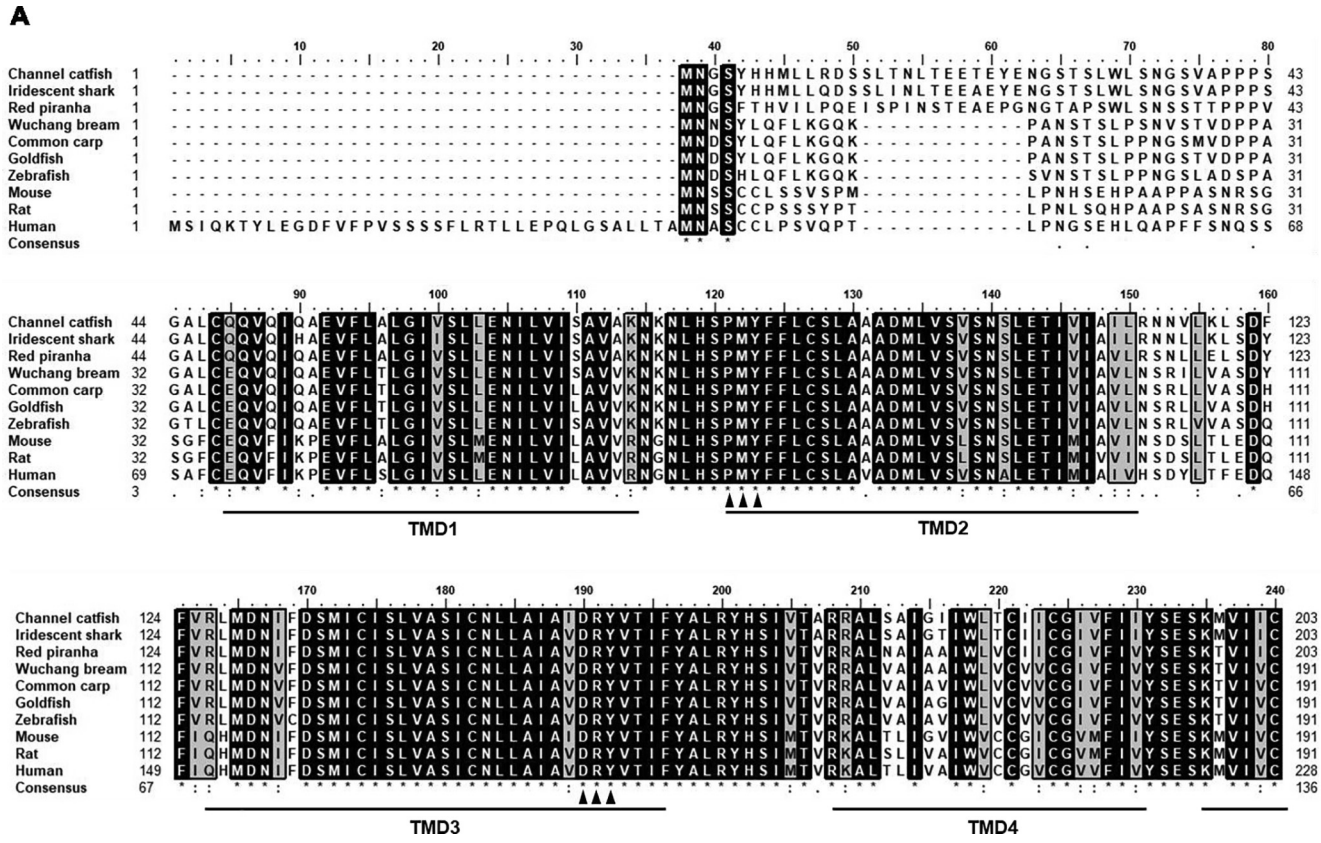

Fig. 2. Comparison of amino acid sequences of MC3R and MRAP2 between channel catfish and other species. (A) Amino acid sequence alignment of MC3Rs. The putative TMDs are marked with lines. PMY, DRY, and DPIIY motifs are indicated by black triangles. (B) Amino acid sequence alignment of MRAP2s. The single putative TMD is underlined. A potential *N*-glycosylation site is indicated. Asterisk (*) denotes the identical amino acid positions. Dot (.) denotes the similar amino acid positions.

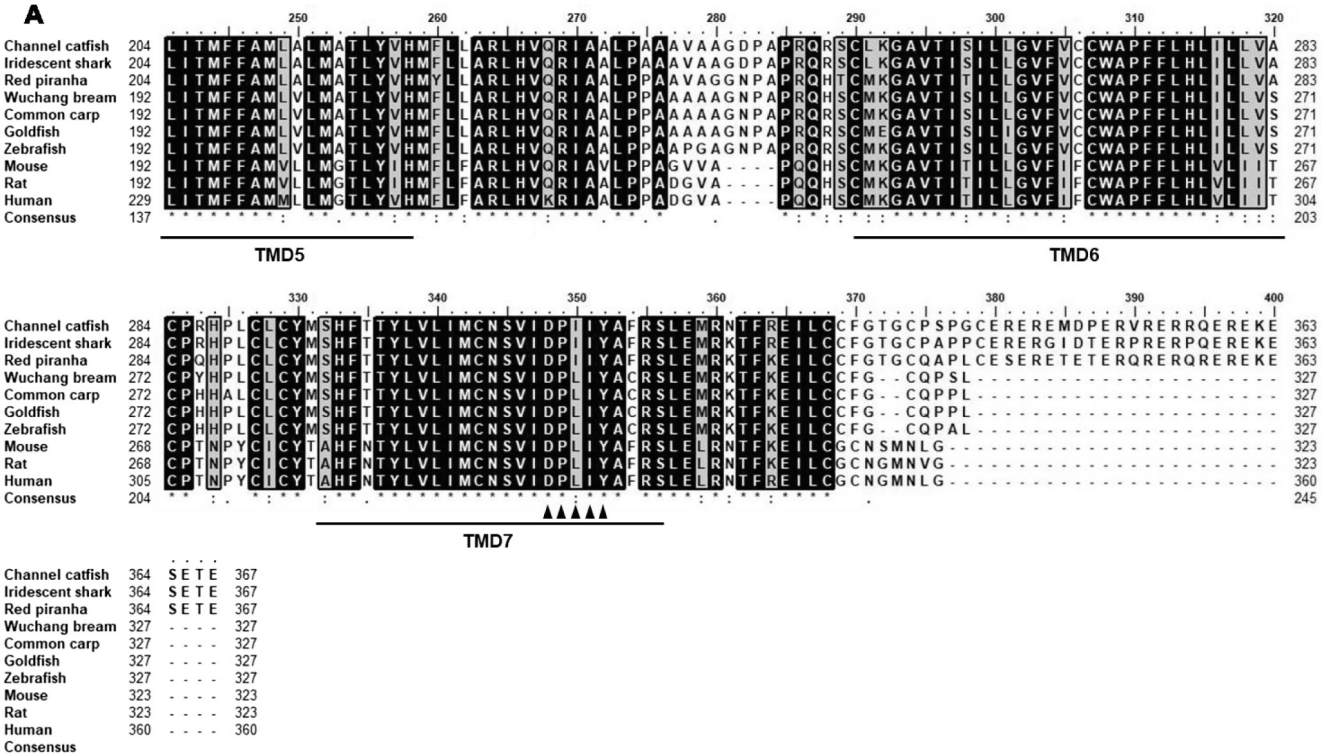

Fig. 2. (*continued*)

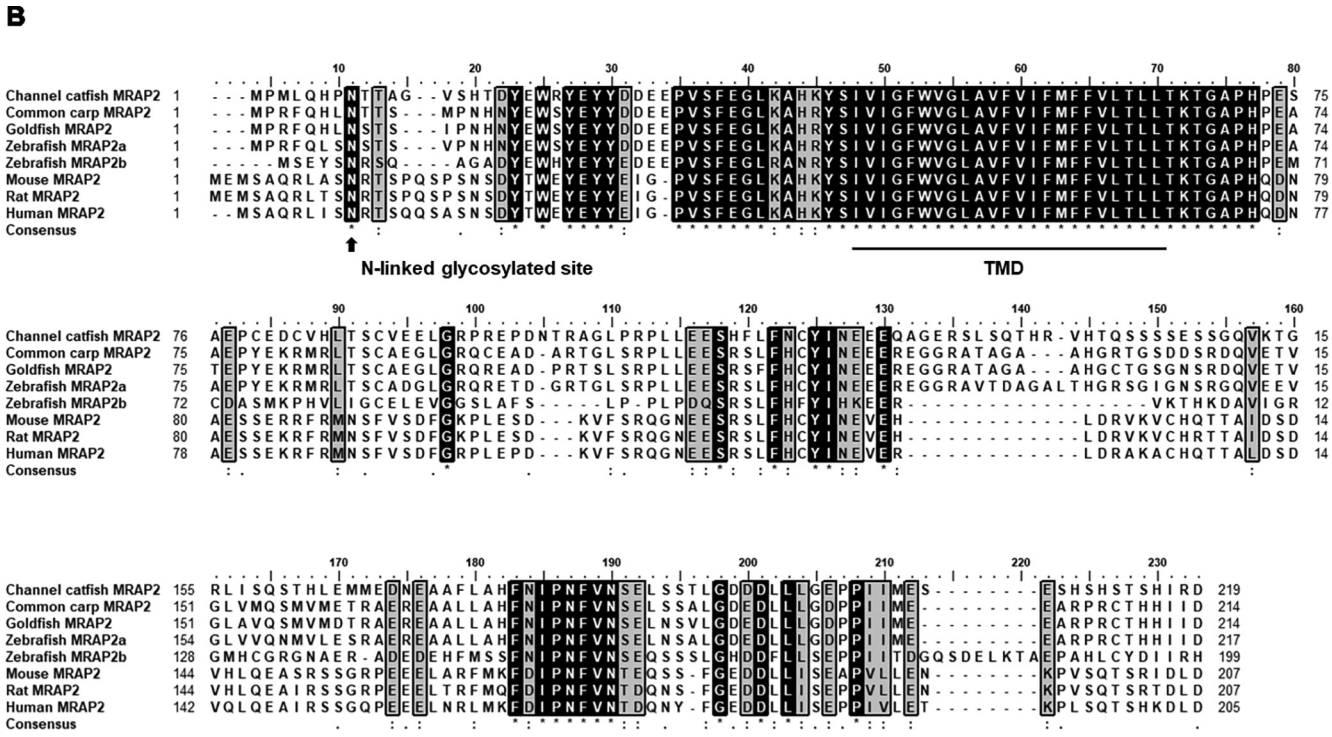

Fig. 2. (*continued*)

catfish has a single intronless *mc3r* gene located on chromosome 5 (Liu et al., 2016). Currently, the approaches for improving the growth and feed efficiency are limited to the use of traditional selective breeding methods that are time consuming. Therefore, understanding of endocrine regulation of energy metabolism in this economically important species can potentially lead to novel approaches to achieve better economic return.

Previous studies have reported the effects of several gut neuropeptides on feeding behavior, glycemia, and hypothalamic *neuropeptide Y* and *pomc* expression in channel catfish (Kobayashi et al., 2008; Peterson et al., 2012; Schroeter et al., 2015), suggesting potential roles of central melanocortin system in the growth and feeding in this fish. In the present study, we investigated the pharmacological properties of channel catfish MC3R (ipMC3R). In addition, the modulatory role of channel catfish MRAP2 (ipMRAP2) on ipMC3R signaling was also studied. These experiments, as the first step towards elucidating the roles of MC3R in energy homeostasis of channel catfish, laid a solid foundation for future physiological studies.

2. Materials and methods

2.1. Ligands and plasmids

[Nle^4, D-Phe^7]-α-MSH (NDP-MSH) and D-Trp^8-γ-MSH were purchased from Peptides International (Louisville, KY, USA). α-MSH and human β-MSH were purchased from Pi Proteomics (Huntsville, AL, USA). Human ACTH (1–24) and AgRP were purchased from Phoenix Pharmaceuticals (Burlingame, CA, USA). [^{125}I]-NDP-MSH and [^{125}I]-cAMP were iodinated using chloramine T method as described in previous publications (Mo et al., 2012; Steiner et al., 1969). The human MC3R (hMC3R) subcloned into pcDNA3.1 vector was generated as previously described (Tao and Segaloff, 2004). The coding sequences of ipMC3R and ipMRAP2 were commercially synthesized and subcloned into pcDNA3.1 vector by GenScript (Piscataway, NJ, USA) to generate the plasmids used for transfection.

2.2. Homology, phylogenetic, and chromosome synteny analyses

Multiple alignments of amino acid sequences of MC3Rs, POMCs, and MRAP2s from different species were performed with BioEdit software using ClustalW multiple alignment. The putative transmembrane domains (TMDs) of ipMC3R were predicted based on the crystal structure of rhodopsin (Palczewski et al., 2000). A phylogenetic tree based on the amino acid sequences was constructed by MEGA X software with 1000 bootstrap replications using the neighbor-joining (NJ) method (Kumar et al., 2018; Saitou and Nei, 1987). Chromosome synteny analysis was performed between several fish and mammalian species with Genomicus (http://www.genomicus.biologie.ens.fr/genomicus) and National Center for Biotechnology Information (NCBI) genome browser (https://www.ncbi.nlm.nih.gov).

2.3. Cell culture and transfection

Human Embryonic Kidney (HEK) 293 T cells (ATCC, Manassas, VA, USA) were cultured in Dulbecco's Modified Eagle's medium (DMEM) (Invitrogen, Carlsbad, CA, USA) containing 10% newborn calf serum (PAA Laboratories, Etobicoke, ON, Canada), 10 mM HEPES, 0.25 μg/mL of amphotericin B, 50 μg/mL of gentamicin, 100 IU/mL of penicillin, and 100 μg/mL of streptomycin at an incubator (37 °C and 5% CO_2-humidified atmosphere). The cells were plated into plates pre-coated with 0.1% gelatin and cultured for about 24 h prior to transfection (24-wells plates for cAMP assays and 6-well plates for ligand binding assay and western blot). At approximately 70% confluency, the cells were transfected or co-transfected with plasmids using calcium phosphate precipitation method (Chen and Okayama, 1987). For ligand binding and signaling assays, ipMC3R (0.25 μg/μL) and hMC3R (0.25 μg/μL) plasmids were transfected into cells, respectively. To study the constitutive activity, ipMC3R plasmids at different concentrations were transfected into cells. To investigate the potential modulation of ipMC3R signaling by ipMRAP2, cells were co-transfected with ipMC3R (0.25 μg/μL) and ipMRAP2 plasmids at different ratios (1:0, 1:1, 1:3, and 1:5). Total plasmid was kept identical for all groups by the addition of empty vector pcDNA3.1.

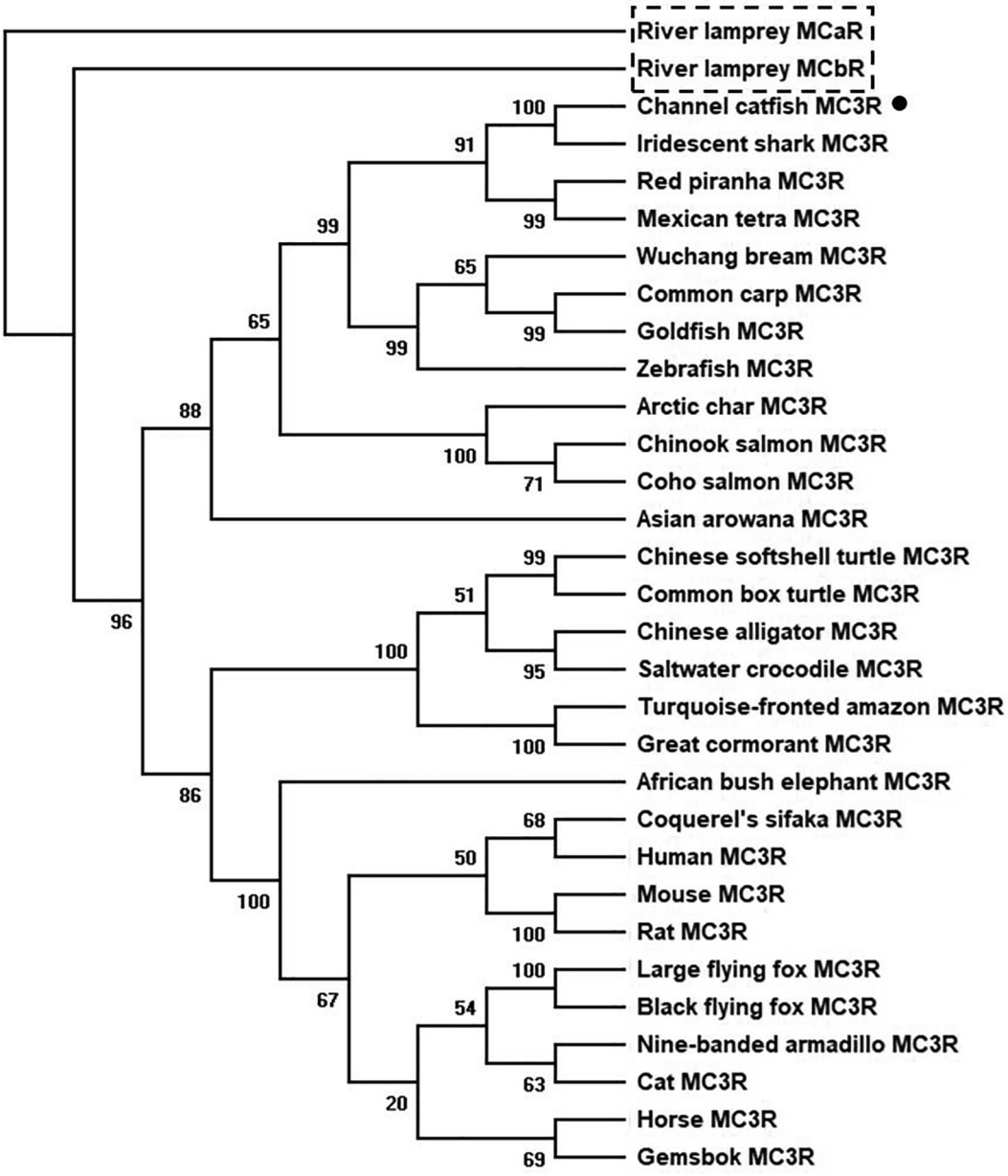

Fig. 3. Phylogenetic tree of MC3Rs. The tree was constructed using the neighbor-joining (NJ) method. Numbers at nodes indicate the bootstrap value, as percentages, obtained for 1000 replicates. Dot indicates ipMC3R. Two river lamprey MCRs (MCaR (ABB36647.1) and MCbR (ABB36648.1)) were used as the outgroups. MC3Rs: channel catfish (XP_017322804.1), iridescent shark (XP_026770221.1), red piranha (XP_017548887.1), Mexican tetra (XP_007231215.1), Wuchang bream (AWA81517.1), common carp (XP_018922723.1), goldfish (BAJ83473.1), zebrafish (NP 851303.2), Chinook salmon (XP 024229914.1), coho salmon (XP_020360426.1), Arctic char (XP_023994975.1), Asian arowana (XP_018615783.1), Chinese softshell turtle (XP_006129463.1), common box turtle (XP_024059166.1), Chinese alligator (XP_006018246.1), saltwater crocodile (XP_019403708.1), turquoise-fronted amazon (KQL61336.1), great cormorant (XP_009512236.1), African bush elephant (XP_003419952.1), sifaka (XP_012501302.1), human (NP_063941.3), mouse (AAI03670.1), rat (NP_001020441.3), large flying fox (XP_011368476.1), black flying fox (XP_006921991.1), nine-banded armadillo (XP_004447768.1), cat (XP_023106851.1), horse (NP_001243901.1), gemsbok (AFH58734.1).

2.4. Ligand binding assay

Forty-eight hours after transfection, HEK293T cells were washed twice with warm DMEM containing 1 mg/mL bovine serum albumin (BSA, EMD Millipore Corporation, Billerica, MA, USA) (DMEM/BSA) and then incubated at 37 °C with DMEM/BSA containing ~80,000 cpm of [^{125}I]-NDP-MSH without or with different concentrations of unlabeled ligands for 1 h (Tao and Segaloff, 2003). The ligands and their final concentrations used in this study were NDP-MSH (10^{-11} to 10^{-6} M), α-MSH (10^{-10} to 10^{-5} M), β-MSH (10^{-10} to 10^{-5} M), ACTH (1–24) (10^{-11} to 10^{-6} M), and D-Trp^{8}-γ-MSH (10^{-11} to 10^{-6} M). After incubation, the plates were placed on ice, and then the cells were washed twice with cold Hank's balanced salt solution containing 1 mg/mL BSA to terminate the reaction. The cells were lysed with 100 μL 0.5 M NaOH and collected using cotton swabs. The radioactivity was counted by a gamma counter (Cobra II Auto-Gamma, Packard Bioscience, Frankfurt, Germany).

2.5. cAMP assay

Forty-eight hours after transfection, HEK293T cells were washed twice with warm DMEM/BSA and then incubated with DMEM/BSA

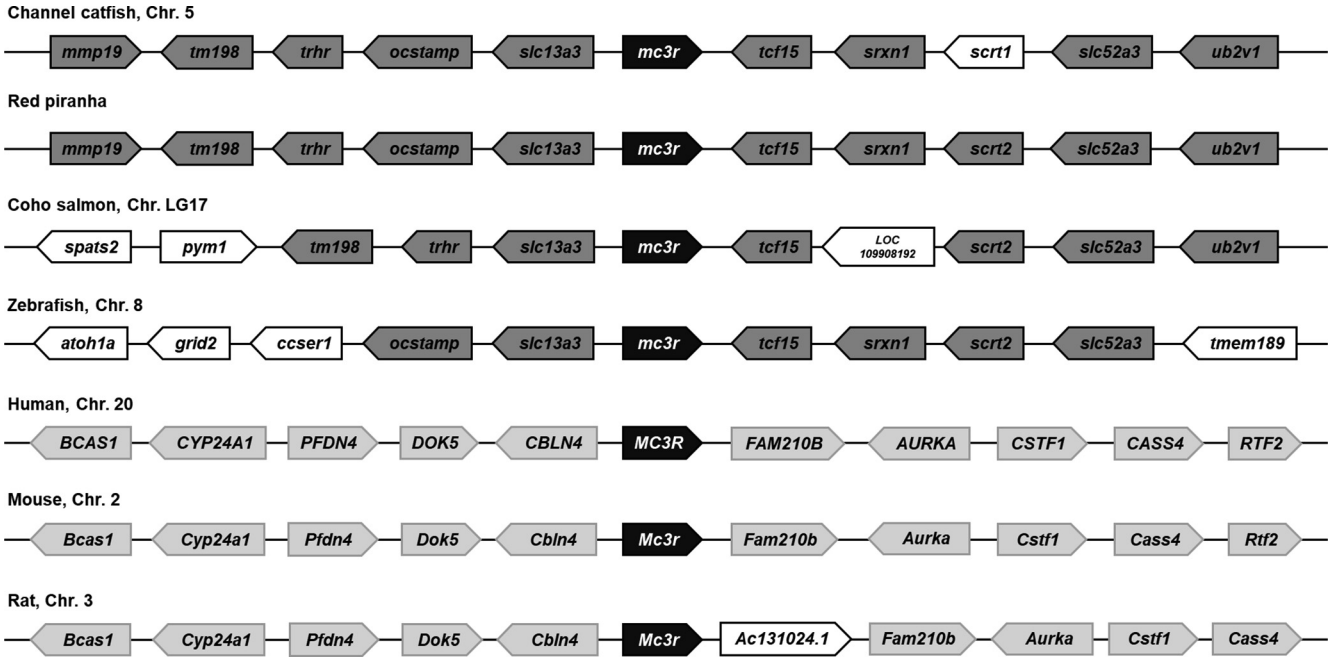

Fig. 4. Chromosomal synteny analyses of *MC3R* genes in different species. The syntenic genes are displayed as boxes with the directions and linked by lines. *MC3R* genes are shown in black boxes. The genes showing conserved synteny in fishes are indicated in dark grey boxes and those in mammals are shown in light grey boxes.

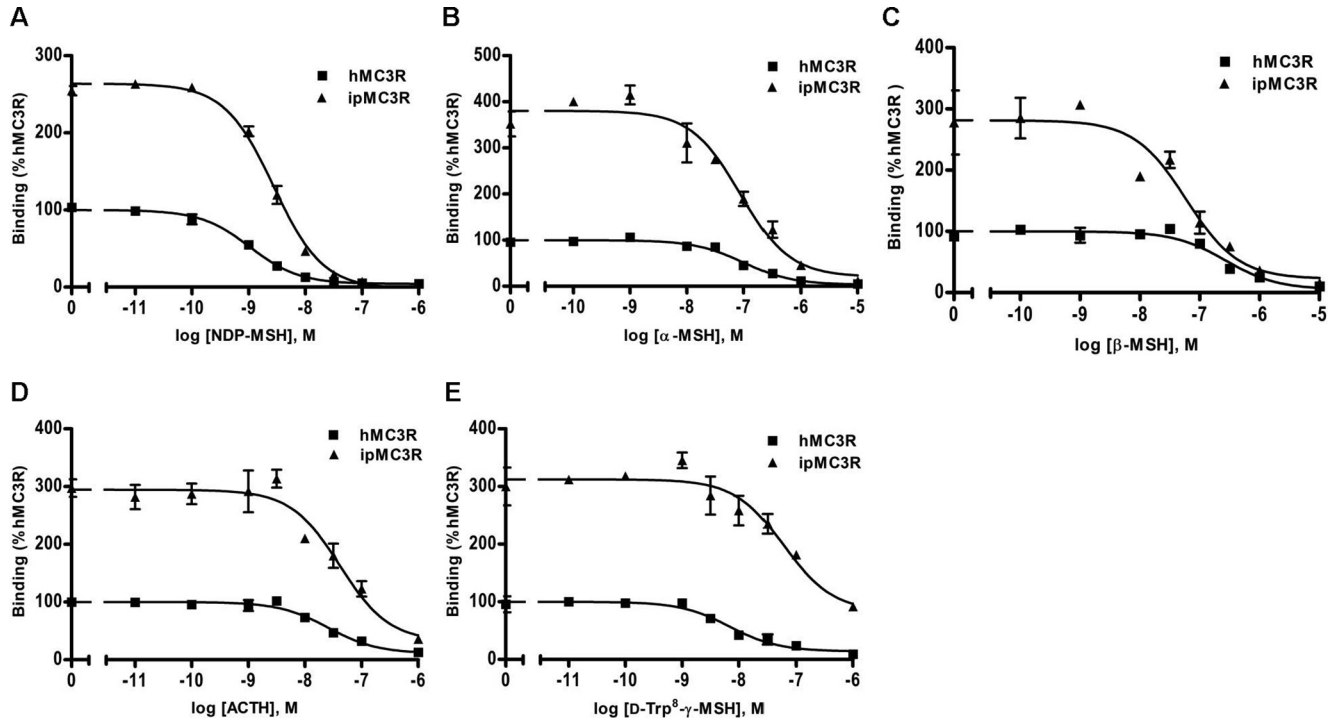

Fig. 5. Ligand binding properties of ipMC3R in HEK293T cells. Different concentrations of unlabeled agonists including (A) NDP-MSH, (B) α-MSH, (C) β-MSH, (D) ACTH (1–24), and (E) D-Trp^{8}-γ-MSH, were used to displace the binding of [^{125}I]-NDP-MSH to MC3Rs in intact cells. Data are expressed as % of hMC3R binding ± range from duplicate measurements within one experiment. The curves are representative of at least three independent experiments.

containing 0.5 mM isobutylmethylxanthine (Sigma–Aldrich, St. Louis, MO, USA) at 37 °C for 30 min. To investigate agonist-stimulated cAMP production, the cells were treated without or with different concentrations of agonists. After one hour incubation at 37 °C, the plates were placed on ice to terminate the reaction, and the cells were lysed with 0.5 M perchloric acid containing 180 μg/mL theophylline (Sigma-Aldrich) and neutralized by 0.72 M KOH/0.6 M $KHCO_3$. The cAMP levels were determined by radioimmunoassay (RIA) as described previously (Steiner et al., 1969).

2.6. ERK1/2 phosphorylation assay

The phosphorylated ERK1/2 (pERK1/2) activity was measured as described previously (He and Tao, 2014; Mo et al., 2012). Briefly, at 24 h after transfection, cells were washed with warm DMEM/BSA once and starved in DMEM/BSA at 37 °C for 24 h. On the day of experiment,

Table 1
The ligand binding properties of ipMC3R.

MC3R	B_{max} (%)	NDP-MSH IC_{50} (nM)	α-MSH IC_{50} (nM)	β-MSH IC_{50} (nM)	ACTH (1–24) IC_{50} (nM)	D-Trp^8-γ-MSH IC_{50} (nM)
hMC3R	100	3.17 ± 1.13	110.91 ± 24.93	309.00 ± 60.51	33.22 ± 5.30	7.91 ± 0.75
ipMC3R	334.01 ± 28.07[b]	5.23 ± 1.27	106.15 ± 17.57	110.33 ± 44.03[a]	53.84 ± 20.37	118.91 ± 29.58[a]

Values are expressed as the mean ± SEM of at least three independent experiments.
[a] Significantly different from the corresponding parameter of hMC3R, $P < 0.05$.
[b] Significantly different from the corresponding parameter of hMC3R, $P < 0.001$.

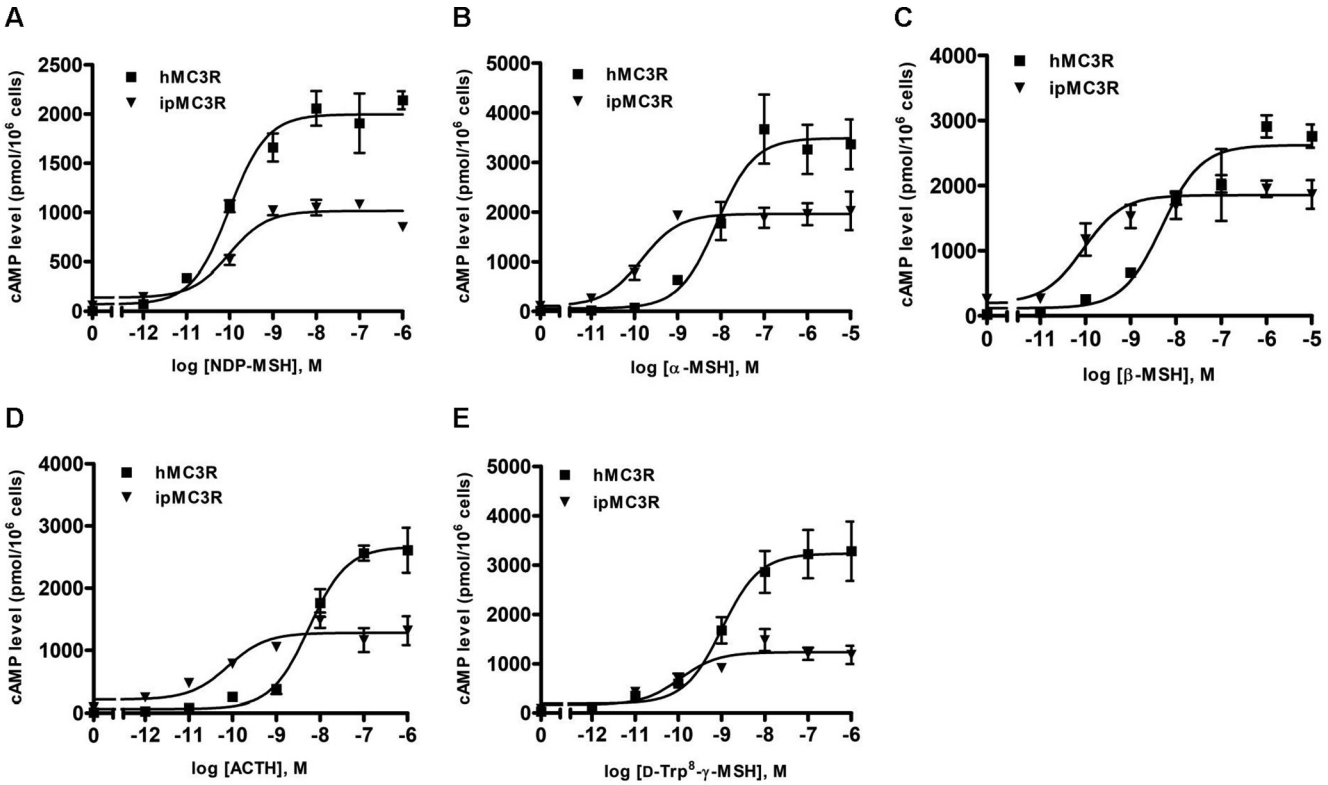

Fig. 6. cAMP signaling properties of ipMC3R in HEK293T cells. Different concentrations of agonists including (A) NDP-MSH, (B) α-MSH, (C) β-MSH, (D) ACTH (1–24), and (E) D-Trp^8-γ-MSH, were used to stimulate cells expressing MC3Rs. The intracellular cAMP levels were measured by RIA. Data are expressed as mean ± SEM from triplicate measurements within one experiment. The curves are representative of at least three independent experiments.

cells were treated with buffer alone or agonists (10^{-6} M α-MSH or 10^{-7} M ACTH (1–24)) for 5 min at 37 °C. Cells were then solubilized in lysis buffer and total protein concentrations of cell lysates were determined using the Bradford protein assay. Samples containing 30 μg of proteins were separated on 10% SDS-PAGE gel and transferred onto PVDF membranes for immunoblotting. Membranes were incubated with 10% non-fat dry milk (containing 0.2% Tween-20) for 4 h at room temperature, and then immunoblotted with rabbit anti-pERK1/2 antibody (Cell Signaling, Beverly, MA) at a dilution of 1:5000, and mouse anti-β-tubulin antibody (Developmental Studies Hybridoma Bank, University of Iowa, Iowa City, IA) at a dilution of 1:5000, in Tris-buffered saline (TBST) containing 0.1% Tween 20 and 5% BSA overnight at 4 °C. Membranes were then incubated with horseradish peroxidase-conjugated secondary antibodies, donkey anti-rabbit IgG (Jackson ImmunoResearch Laboratories, West Grove, PA) at a dilution of 1:8000 and donkey anti-mouse IgG (Jackson ImmunoResearch Laboratories) at a dilution of 1:10000 in 10% non-fat dry milk (containing 0.2% Tween-20) for one hour at room temperature. Specific bands were visualized using enhanced chemiluminescence reagent (Thermo Scientific, Rockford, IL) and staining intensity was quantified using ImageJ Software (National Institute of Health, Bethesda, MD). The pERK1/2 levels were normalized according to the loading of proteins by expressing the data as a ratio of pERK1/2 over β-tubulin.

2.7. Statistical analysis

All data were presented as mean ± SEM. GraphPad Prism 4.0 software (San Diego, CA, USA) was used to calculate parameters in ligand binding and cAMP signaling assays. Two-tailed Student's *t*-test was performed to determine the significant differences in ligand binding and signaling parameters between hMC3R and ipMC3R, basal cAMP levels between AgRP-treated and non-treated groups, and pERK1/2 levels between agonist-treated and non-treated groups. One-way analysis of variance (one-way ANOVA) and two-way analysis of variance (two-way ANOVA) were performed in the investigation of ipMRAP2 effects on ipMC3R signaling. Statistical significance was established when $P < 0.05$.

3. Results

3.1. Sequence analyses of ipMC3R, ipPOMC, and ipMRAP2

The catfish *mc3r* gene contained an open reading frame of 1104 bp (NCBI, XM_017467315.1) encoding a putative protein of 367 amino

Table 2
The cAMP signaling properties of ipMC3R.

MC3R	Basal (%)	NDP-MSH		α-MSH		β-MSH		ACTH (1–24)		D-Trp8-γ-MSH	
		EC_{50} (nM)	R_{max} (%)	EC_{50} (nM)	R_{max} (%)	EC_{50} (nM)	R_{max} (%)	EC_{50} (nM)	R_{max} (%)	EC_{50} (nM)	R_{max} (%)
hMC3R	100	0.29 ± 0.15	100	8.82 ± 1.99	100	7.52 ± 0.99	100	4.89 ± 0.87	100	1.47 ± 0.31	100
ipMC3R	695.81 ± 83.67[c]	0.48 ± 0.20	61.44 ± 6.00[c]	0.24 ± 0.11[a]	69.41 ± 10.50[a]	0.10 ± 0.02[c]	65.64 ± 3.42[c]	0.15 ± 0.07[b]	68.45 ± 13.14[a]	0.32 ± 0.14[a]	53.18 ± 9.40[b]

Values are expressed as the mean ± SEM of at least three independent experiments. The basal cAMP level of hMC3R was 15.74 ± 1.63 pmol/10^6 cells. The maximal response (R_{max}) values of hMC3R were 2514.80 ± 541.54, 2882.33 ± 329.29, 2267.50 ± 470.49, 2873.80 ± 547.63, and 2514.67 ± 357.79 pmol/10^6 cells upon NDP-MSH, α-MSH, β-MSH, ACTH (1–24), and D-Trp^8-γ-MSH stimulation, respectively.

[a] Significantly different from the corresponding parameter of hMC3R, $P < 0.05$.
[b] Significantly different from the corresponding parameter of hMC3R, $P < 0.01$.
[c] Significantly different from the corresponding parameter of hMC3R, $P < 0.001$.

acids (NCBI, XP_017322804.1) and 41.05 kDa molecular mass (Fig. 1). Multiple alignment of MC3Rs revealed that the predicated ipMC3R had the classical feature of Family A GPCRs, with seven hydrophobic TMDs and several conserved motifs (PMY, DRY, and DPIIY) at homologous positions with MC3Rs of other species. The deduced amino acid sequence of ipMC3R was significantly conserved to other species in the TMDs, intracellular loops, and extracellular loops, but the amino and carboxyl termini displayed the lowest identities to other species (Fig. 2A). The identities between ipMC3R and other piscine MC3R orthologs were 95% (iridescent shark, *Pangasianodon hypophthalmus*), 84% (red piranha, *Pygocentrus nattereri*), 81% (Wuchang bream, *Megalobrama amblycephala*), 81% (common carp, *Cyprinus carpio*), 81% (goldfish, *Carassius auratus*), and 80% (zebrafish, *Danio rerio*). However, ipMC3R had lower identities with mammalian MC3Rs (70% to mouse, 69% to rat, and 67% to human).

POMC is the precursor of several melanocortins including α-, β-, γ-MSH and ACTH. In humans and rodents, all melanocortins share the pharmacophore (HFWR) that is necessary to bind to MCRs. Consistent with one previous study identifying *pomc* gene in channel catfish (Karsi et al., 2004), multiple alignment of amino acid sequences of POMCs in this study also suggested that α-MSHs, β-MSHs, and ACTHs might exist in channel catfish and other fishes with potential absence of γ-MSHs (the core sequence was not found in the region that is supposed to produce γ-MSH) (Supplementary Fig. 1). Although there were differences in the sequences of ACTH and β-MSH (74% and 59% identity between human and catfish ACTH and β-MSH, respectively), it is interesting to note that α-MSH of channel catfish was identical to those of other fish and mammals, indicating that α-MSH is highly conserved in structure during evolution and potentially functions similarly in both mammals and fish (Supplementary Fig. 1).

The ipMRAP2 was also highly conserved with an identical TMD in the species analyzed (Fig. 2B). We did not find MRAP1 sequence in channel catfish based on the genome data, suggesting the absence of this gene in channel catfish.

3.2. Phylogenetic and chromosome synteny analyses of ipMC3R

Phylogenetic analysis was conducted with full-length amino acid sequences of ipMC3R and other MC3Rs to evaluate the evolutionary relationships between the predicted ipMC3R and other vertebrate MC3Rs. We showed that ipMC3R was nested within a clade of iridescent shark, red piranha and Mexican tetra (Fig. 3). Chromosome synteny analysis also revealed that ipMC3R was orthologous to those of other fishes. The *mc3r* gene neighbors exhibited a conserved synteny to those of red piranha, coho salmon, and zebrafish, but not to those of human, mouse, and rat (Fig. 4).

3.3. Ligand binding properties of ipMC3R

Competitive ligand binding assay was performed to investigate the binding properties of ipMC3R to different MC3R ligands, including three endogenous agonists (α-MSH, β-MSH, and ACTH (1–24)), one superpotent agonist (NDP-MSH), and one MC3R-selective agonist (D-Trp^8-γ-MSH) (Grieco et al., 2000). Different concentrations of unlabeled ligands were used to compete for radiolabeled ligand ([^{125}I]-NDP-MSH) binding. In the same experiments, we included hMC3R for comparison to see whether ipMC3R has any unique pharmacological characteristics. As shown in Fig. 5 and Table 1, the maximal binding value (B_{max}) of ipMC3R was 334 ± 28% of that of the hMC3R ($P < 0.01$). The two MC3Rs had similar IC_{50}s when NDP-MSH, α-MSH, and ACTH (1–24) were used to compete for [^{125}I]-NDP-MSH binding. However, ipMC3R had significantly higher and lower affinities to β-MSH and D-Trp^8-γ-MSH, respectively.

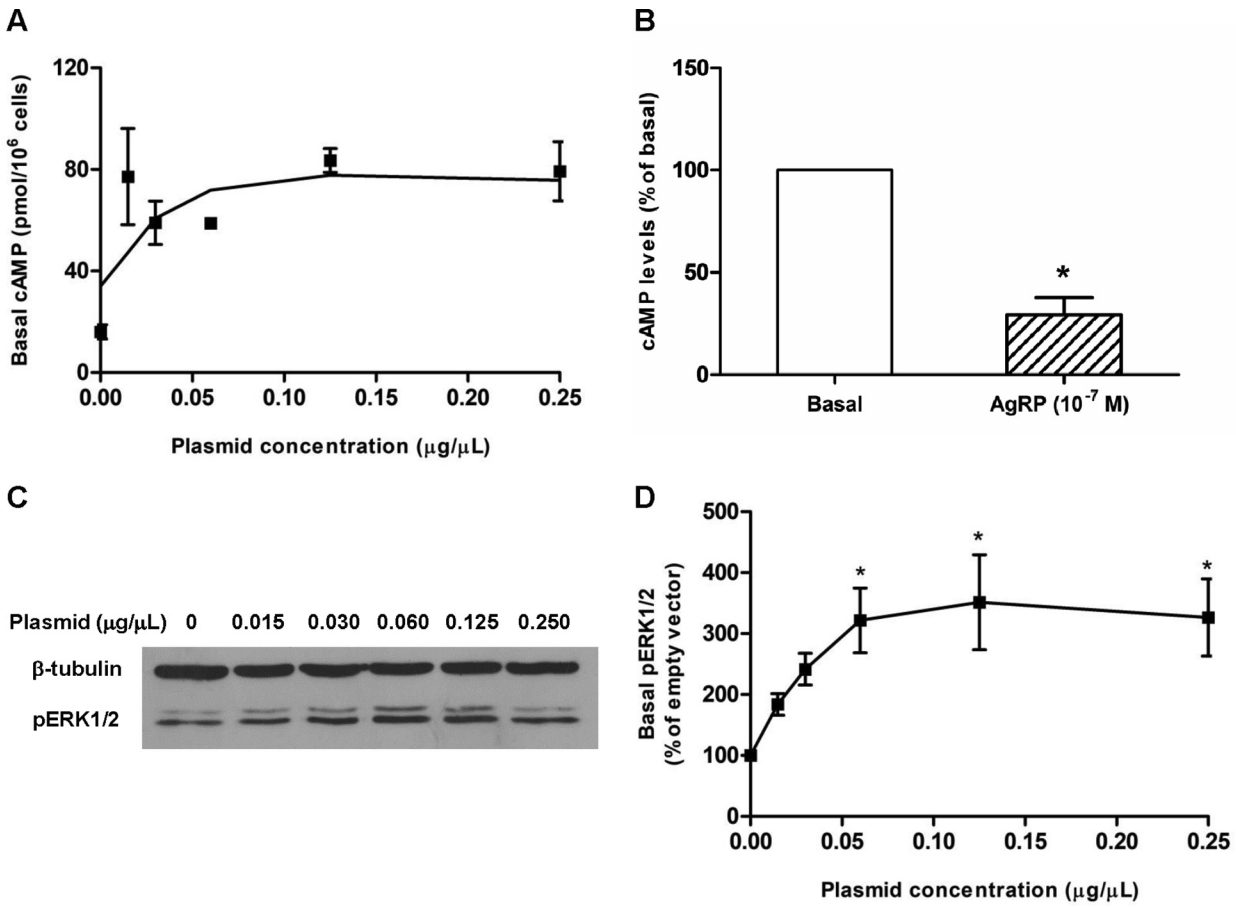

Fig. 7. Constitutive activities of ipMC3R in both cAMP and ERK1/2 pathways. (A) The cAMP levels of HEK293T cells transfected with increasing concentrations of ipMC3R plasmids were measured by RIA. The curve is representative of three independent experiments. (B) HEK293T cells transfected with ipMC3R (plasmid concentration: 0.25 μg/μL) were treated without or with 10^{-7} M AgRP. The intracellular cAMP levels were measured by RIA. The data are expressed as mean ± SEM from three independent experiments. Asterisk (*) indicates significant difference between control and ligand treatment (two-tailed Student's *t*-test). (C) The ERK1/2 phosphorylation levels of HEK293T cells transfected with increasing concentrations of ipMC3R plasmids were measured by western blot. (D) Values are expressed as mean ± SEM of five independent experiments. Asterisk (*) indicates significant difference from the basal ERK1/2 phosphorylation level of cells transfected with empty pcDNA3.1 vector (One-way ANOVA followed by Dunnett test). In (A), (C), and (D), different concentrations of empty vector pcDNA3.1 were added to maintain the identical total plasmid amount.

3.4. Signaling properties of ipMC3R

RIA was performed to determine whether ipMC3R could respond to these agonists in cAMP pathway. All agonists were shown to dose-dependently stimulate ipMC3R and increase intracellular cAMP generation. Cells transfected with empty vector pcDNA3.1 alone did not respond to agonist stimulation (Supplementary Fig. 2). As shown in Fig. 6 and Table 2, the maximal responses of ipMC3R to the five agonists were significantly lower (~50% to 70% of hMC3R). The EC_{50} of NDP-MSH for ipMC3R was comparable to that of the hMC3R (Fig. 6A and Table 2), whereas the EC_{50}s of α-MSH, β-MSH, ACTH (1–24), and D-Trp^8-γ-MSH for ipMC3R were significantly lower than those of hMC3R (Fig. 6B–E, and Table 2).

3.5. Constitutive activity of ipMC3R

In this experiment, we also found the basal cAMP level of ipMC3R was 7-fold higher than that of hMC3R (109.52 ± 13.17 vs. 15.74 ± 1.63 pmol/10^6 cells, n = 20), suggesting that ipMC3R might be constitutively active. To further study the constitutive activity of ipMC3R, we transfected cells with increasing concentrations of plasmid. Empty vector pcDNA3.1 was used to normalize the amount of DNA added to each well. Our data showed that even very low amount of ipMC3R plasmid transfected resulted in high basal cAMP levels (Fig. 7A). The high basal cAMP level at plasmid concentration of 0.25 μg/mL could be reduced by AgRP by 63.83% (Fig. 7B), suggesting that AgRP was a potent inverse agonist at ipMC3R.

In addition to cAMP pathway, ERK1/2 signaling was also evaluated. ERK1/2 phosphorylation increased with increasing concentrations of plasmid transfected (Fig. 7C and D), suggesting that ipMC3R was also constitutively active in the ERK1/2 pathway.

3.6. Modulation of ipMC3R signaling by ipMRAP2

In the present study, we investigated the actions of ipMRAP2 on ipMC3R signaling. Cells were co-transfected with ipMC3R and ipMRAP2 at different ratios (1:0, 1:1, 1:3, and 1:5). Our results showed that ipMRAP2 could dose-dependently reduce the basal cAMP levels with maximal inhibition observed at the 1:5 ratio (56.66% of 1:0 group) (Fig. 8A). Significant reduction in agonist-induced cAMP generation was also observed (Fig. 8B and C). To further explore the mechanism, cells co-transfected with ipMC3R and ipMRAP2 at the ratios of 1:0 and 1:5 were stimulated with different concentrations of α-MSH. We showed that ipMRAP2 significantly reduced the maximal response by ~25%, whereas it did not affect the EC_{50} significantly (Fig. 8D).

In addition to cAMP production, both α-MSH and ACTH (1–24) could activate ERK1/2 pathway through ipMC3R (Fig. 9A and B). Cells transfected with empty vector pcDNA3.1 or ipMRAP2 alone did not

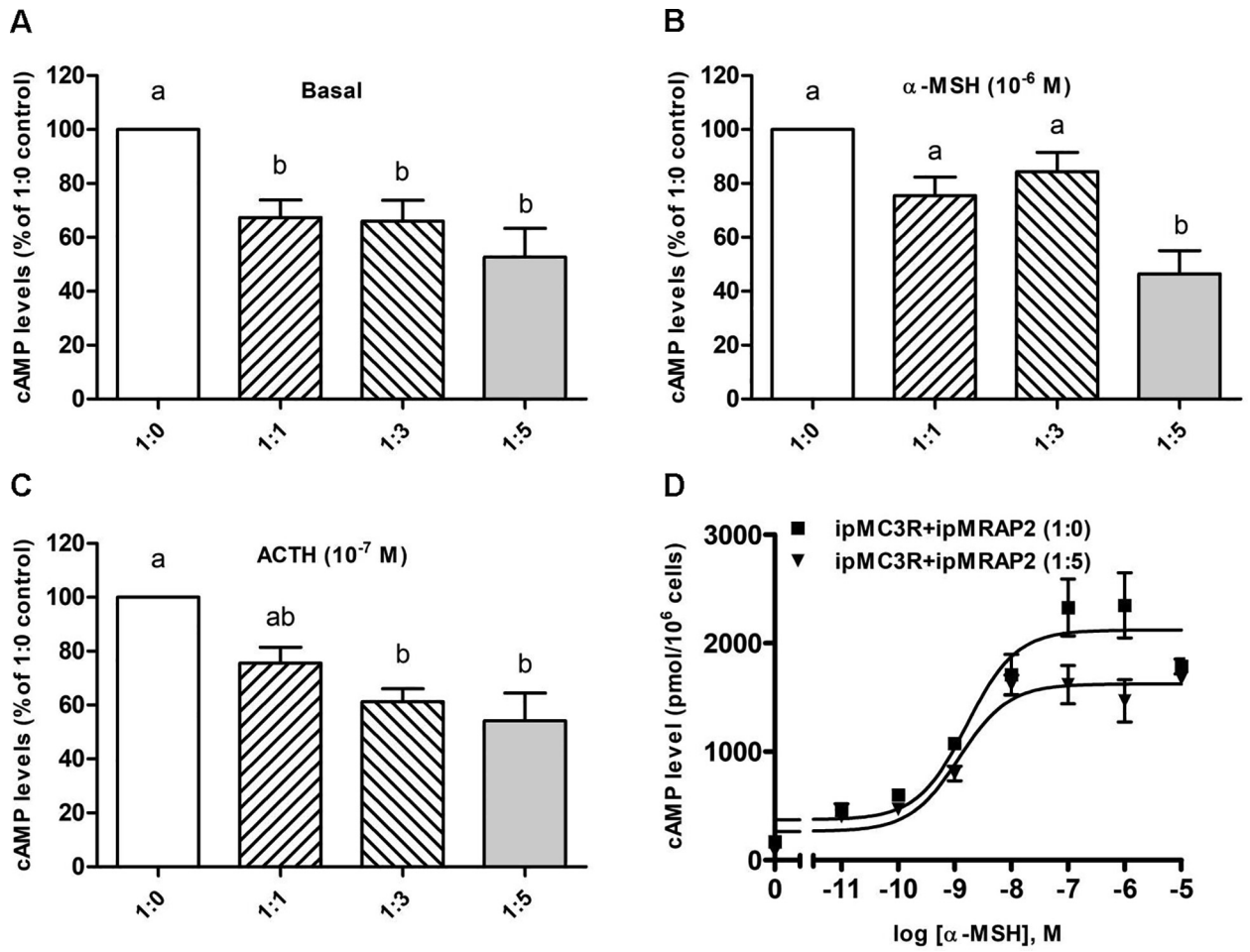

Fig. 8. The actions of ipMRAP2 on cAMP signaling of ipMC3R in HEK293T cells. The cAMP levels of ipMC3R stimulated without (A) or with agonists α-MSH (B) and ACTH (1–24) (C), could be dose-dependently inhibited by ipMRAP2. Values are expressed as mean ± SEM of four independent experiments. Values marked with different lowercase letters are significantly different (One-way ANOVA followed by Tukey test). (D) The curve is representative of five independent experiments in which different concentrations of α-MSH were used to stimulate cells co-transfected with ipMC3R and ipMRAP2 at the ratios of 1:0 and 1:5.

respond to α-MSH and ACTH (1–24) stimulation (Fig. 9A and B). When ipMRAP2 were coexpressed with ipMC3R, ipMRAP2 had no effect on basal and α-MSH- and ACTH (1–24)-stimulated pERK1/2 levels (Fig. 9C and D), different from its actions on cAMP pathway (Fig. 8).

4. Discussion

The MC3Rs have been extensively studied in human and rodents regarding their roles in regulating energy balance (such as regulation of feed efficiency and nutrient partitioning, maintaining circadian rhythm, and adaptation to fasting and overfeeding) as well as modulation of immune response. Several groups also functionally studied MC3Rs in some other mammals and non-mammalian vertebrates (Fan et al., 2008; Zhang et al., 2019, 2017). Given the critical functions of MC3Rs in regulation of energy homeostasis, it is also important to understand the roles of MC3Rs in economically important aquaculture fishes. However, to our knowledge, only a few studies investigated MC3Rs in fishes, such as spiny dogfish (Klovins et al., 2004b) and red stingray (Takahashi et al., 2016). In the present study, we characterized channel catfish MC3R by performing several pharmacological and functional studies, aiming to lay a foundation for future physiological studies that could provide new strategies for enhancing channel catfish culture.

We found that ipMC3R had a typical structure of family A GPCR, similar as MC3Rs of other species (Figs. 1 and 2A). The ipMC3R showed a remarkable conservation with several other teleost MC3Rs at the amino acid level (more than 80% identities). Seven TMDs were present in ipMC3R, which were highly conserved among MC3Rs from different species. Several highly conserved motifs that are known to be important for receptor structure and function, such as PMY in TMD2, DRY in TMD3, and DPIIY in TMD7, were also identified in ipMC3R. It is interesting to note that ipMC3R had a long C-terminal domain similar as in iridescent shark and red piranha but different from those in other fish and mammalian MC3Rs (Fig. 2A), which might account for its unique properties. The ipMC3R was also evolutionarily conserved since phylogenetic tree revealed that ipMC3R was clustered with teleost MC3Rs and chromosomal synteny analysis showed that the surrounding genes of catfish *mc3r* were similar to those in red piranha, coho salmon, and zebrafish (Figs. 3 and 4).

To investigate the pharmacology of ipMC3R, we first performed competitive ligand binding assays in HEK293T cells transfected with ipMC3R plasmid. As shown in Fig. 5 and Table 1, the super-potent agonist NDP-MSH bound to ipMC3R with the highest affinity, comparable to that of hMC3R. The binding affinities of ipMC3R to α-MSH or ACTH (1–24) were also comparable to those of hMC3R. Significant 15-fold difference is observed between IC_{50}s of hMC3R and ipMC3R when D-Trp^8-γ-MSH, an analogue of γ-MSH, was used (Fig. 5E and Table 1). In mammals, among the five subtypes of MCRs, MC3R has the highest affinity to γ-MSH and is the only MCR that is fully activated by γ-MSH (Cone, 2006). However, potential γ-MSH region was not found in channel catfish POMC (Karsi et al., 2004) (Supplementary Fig. 1). Therefore, the low affinity of D-Trp^8-γ-MSH to ipMC3R might be explained by the absence of γ-MSH in this species.

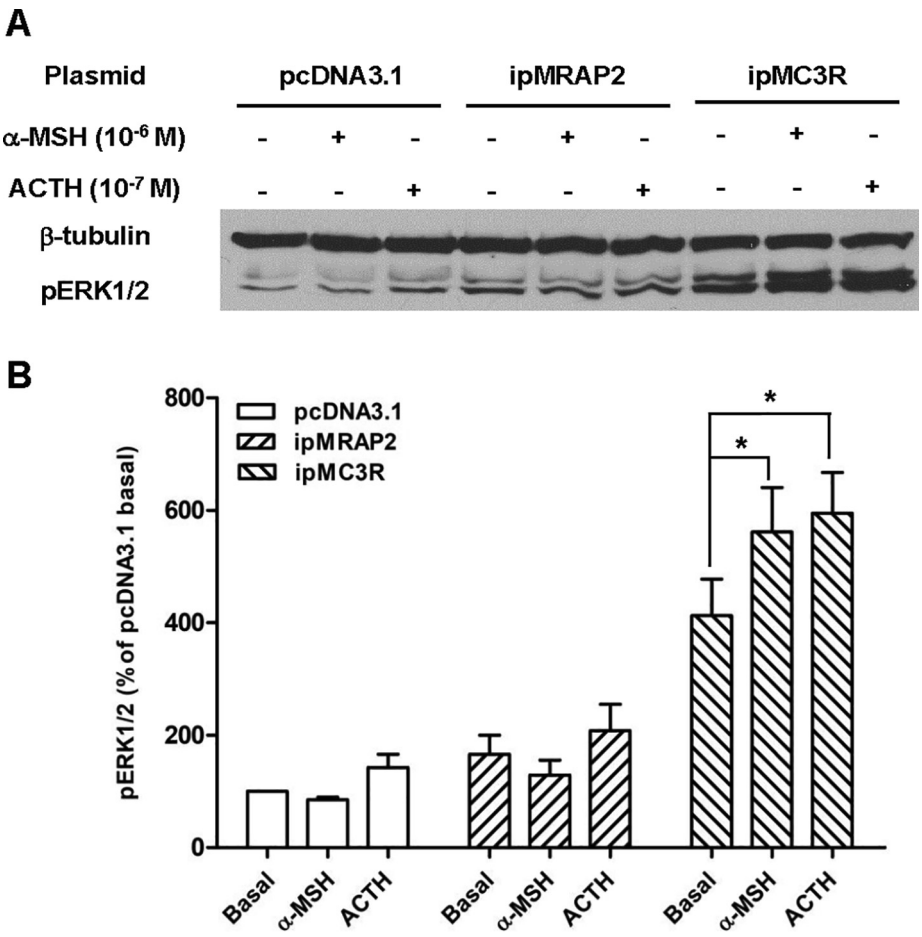

Fig. 9. The actions of ipMRAP2 on ERK1/2 signaling of ipMC3R in HEK293T cells. (A and B) Cells transfected with empty vector pcDNA3.1, ipMRAP2, and ipMC3R were stimulated without or with α-MSH and ACTH (1–24). The ERK1/2 phosphorylation levels were measured by western blot. Asterisk (*) indicates significant difference from the each basal ERK1/2 phosphorylation level (Two-tailed Student's *t*-test). (C and D) Cells co-transfected with ipMC3R and ipMRAP2 at different ratios were stimulated without or with α-MSH and ACTH (1–24). The ERK1/2 phosphorylation levels were measured by western blot. Hash symbol (#) indicates that the ERK1/2 phosphorylation of all ligand-treated groups are significantly different from those of the corresponding control groups (two-way ANOVA followed by Bonferroni test). All values are expressed as mean ± SEM of at least five independent experiments.

The MC3R couples to both Gs-cAMP and ERK1/2 pathways. We next investigated the signaling properties of ipMC3R on both cAMP production and ERK1/2 activation. In cAMP assays, our data showed that the maximal responses of ipMC3R to five agonists were about 50 to 70% of those of hMC3R (Fig. 6 and Table 2). In addition, all five agonists could stimulate ipMC3R with sub-nanomolar potencies. In particular, the sub-nanomolar potency of ACTH (1–24) at ipMC3R, significantly different from its nanomolar potency at hMC3R (Fig. 6D, and Table 2), indicated that ACTH might be an important endogenous ligand for ipMC3R. ACTH was proposed as the "original" ligand for the early MCRs during vertebrate evolution, since ACTH could bind to and/or stimulate MC4R with high affinity and/or potency in several fishes (Haitina et al., 2004; Klovins et al., 2004a; Li et al., 2016, 2017; Yi et al., 2018). Only one study reported the results on the MC3R (Klovins et al., 2004b). Our results showing the high affinity and potency of ACTH (1–24) to ipMC3R provide further support for the importance of ACTH as an endogenous ligand for fish MC3R.

As another pathway triggered by MC3R, ERK1/2 activation was shown to be involved in the regulation of energy homeostasis in terms of food intake, feeding behaviors and long-lasting effects of melanocortins (Begriche et al., 2012; Daniels et al., 2003; Sutton et al., 2005). In this study, ERK1/2 activation was also observed when cells were stimulated by α-MSH and ACTH (1–24) (Fig. 9A and B), suggesting that ipMC3R might trigger ERK1/2 pathway similar to hMC3R, thus contributing to the regulation of energy homeostasis.

Previous studies showed that several fish MC4Rs are constitutively active in cAMP pathway (Li et al., 2016, 2017; Sanchez et al., 2009; Sebag et al., 2013; Yi et al., 2018). In cavefish, mutations of *mc4r* leading to decreased constitutive activity was considered as one cause of elevated appetite, growth, and starvation resistance, suggesting the physiological relevance of constitutive activity (Aspiras et al., 2015). Only zebrafish MC3R was shown to be constitutively active in the cAMP pathway before (Renquist et al., 2013). We revealed that ipMC3R displayed constitutive activity in cAMP pathway (Fig. 7A and Table 2) in contrast to hMC3R which has little or no constitutive activity in this pathway (Tao, 2007; Tao et al., 2010). AgRP is orexigenic in fishes (reviewed in (Volkoff, 2016)). The high basal cAMP level of ipMC3R could be potently reduced by AgRP (Fig. 7B) in accordance with the findings in chicken and zebrafish MC3Rs (Renquist et al., 2013; Zhang et al., 2017), indicating that AgRP was also a potent inverse agonist for ipMC3R. Therefore AgRP could potentially regulate energy balance through MC3R in channel catfish. Furthermore, we showed that ipMC3R was also constitutively active in ERK1/2 pathway (Fig. 7C and D).

In mammals, MRAP1 is highly expressed in the adrenal gland with the indispensable function in trafficking MC2R to the plasma membrane. Mutations in *MRAP1* accounts for ~20% of cases of familial glucocorticoid deficiency type 2 and causes earlier disease onset compared with familial glucocorticoid deficiency type 1 resulting from mutations in *MC2R* (Chung et al., 2010; Metherell et al., 2005).

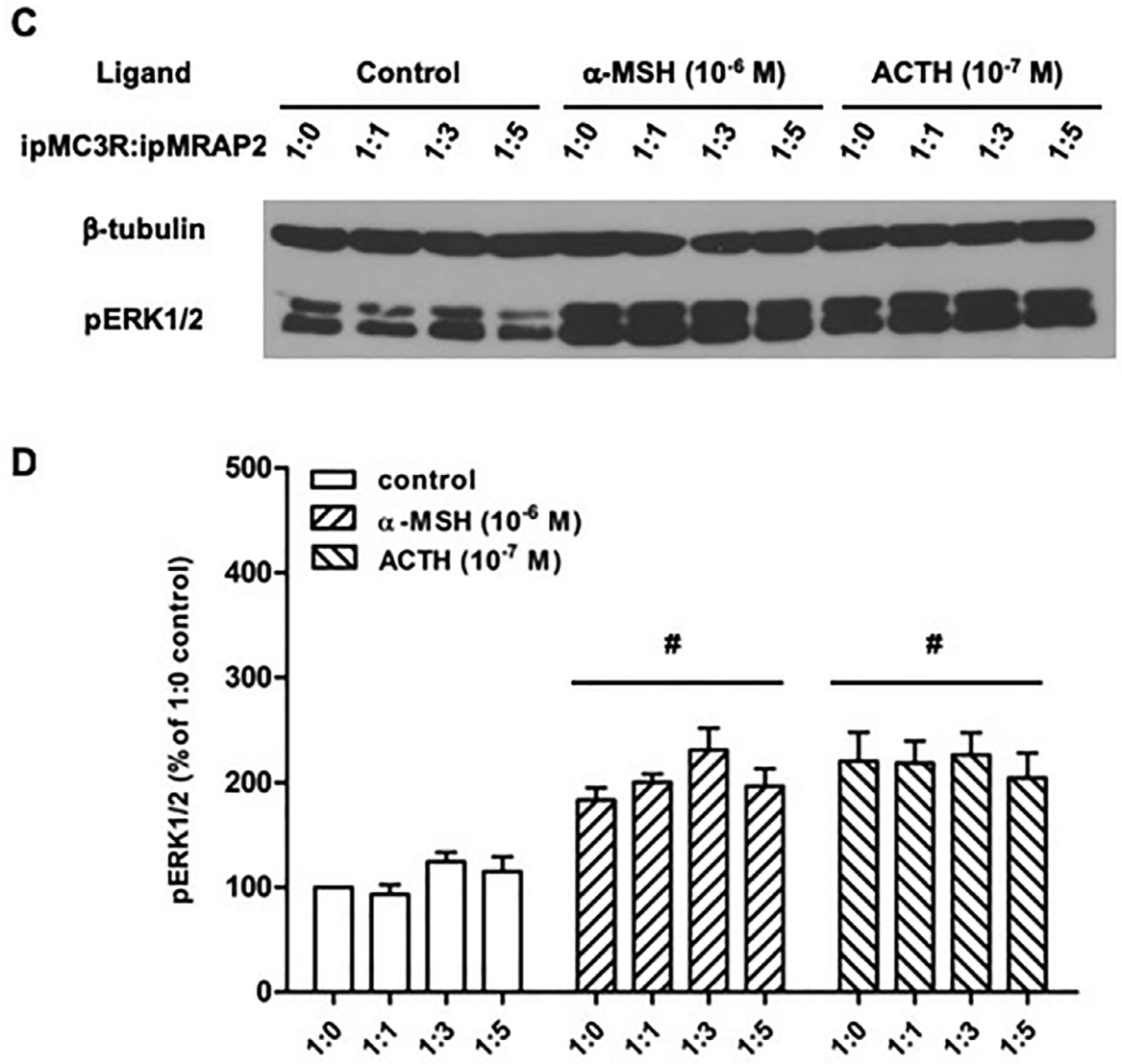

Fig. 9. (*continued*)

Different from MRAP1, MRAP2 is primarily expressed in the hypothalamus and has impact on regulation of energy homeostasis through interaction with MC4R (Asai et al., 2013; Sebag et al., 2013), as well as prokineticin receptors (Chaly et al., 2016) and ghrelin receptor (Srisai et al., 2017). Mice with *Mrap2* deletion display severe obesity (Asai et al., 2013). Potentially pathogenic *MRAP2* mutations have also been identified in humans with obesity (Asai et al., 2013), which impair the function of MC4R and thus lead to obesity. In zebrafish, MC4R signaling can be differentially modulated by two isoforms of MRAP2, MRAP2a and MRAP2b, leading to distinct regulation on energy homeostasis (Sebag et al., 2013). MRAP2a stimulates growth of zebrafish by strongly inhibiting MC4R signaling, whereas MRAP2b increases ligand sensitivity and potentiates MC4R signaling (Sebag et al., 2013).

As for the MC3R, there are only three previous studies reporting the modulation of signaling by MRAPs (Chan et al., 2009; Kay et al., 2013; Zhang et al., 2017). The first study showed that in CHO cells expressing hMC3R, human MRAP2 significantly reduces NDP-MSH-induced cAMP production (Chan et al., 2009). Kay et al. showed that hMRAPa increases agonist-induced signaling (Kay et al., 2013). Zhang et al. demonstrated that in chicken MC3R, MRAP2 decreases constitutive activity but potentiates agonist-induced signaling in the cAMP pathway (Zhang et al., 2017). In the present study, we investigated the role of ipMRAP2 in modulating ipMC3R signaling in both cAMP and ERK1/2 pathways. As shown in Fig. 8, ipMRAP2 inhibited both constitutive and agonist-induced signaling in cAMP pathway. However, the constitutive activity and agonist-induced ERK1/2 activation in ERK1/2 pathway were not affected (Fig. 9C and 9D). We suggest that ipMRAP2 preferentially stabilized ipMC3R in an inactive conformation for cAMP production but not ERK1/2 activation.

In the present study, we used a mammalian cell line cultured at 37 °C to perform the pharmacological studies. Although this is a widely used strategy, partly due to the lack of well-established piscine cell expression system, we caution that the activities of fish receptors may potentially be affected by the properties of the mammalian cells and culture temperature, such as different viscosities of cell membrane at different temperatures. Viscosity is known to affect receptor conformational changes and downstream adenylyl cyclase activity (Hirata et al., 1979).

In summary, we showed that ipMC3R was evolutionarily conserved in piscine MC3Rs. The cloned ipMC3R was a functional receptor with unique pharmacological properties compared to hMC3R, such as high constitutive activities and high sensitivities to α-MSH and ACTH (1–24). We also showed that ipMRAP2 could preferentially modulate the cAMP signaling rather than ERK1/2 pathway. Therefore, we proposed that MC3R, melanocortins (α-MSH and ACTH), and MRAP2, as well as inverse agonist AgRP, are important components in a complex

network that contribute to the central regulation of energy homeostasis in channel catfish. Novel strategies might be developed targeting each of these components to improve the growth and quality of this cultured fish.

Acknowledgments

This study was supported by a grant from Ocean University of China – Auburn University Joint Research Center for Aquaculture and Environmental Science and the Fundamental Research Funds for the Central Universities in China (841712004). Li-Kun Yang and Zheng-Rui Zhang received graduate fellowships from China Scholarship Council, People's Republic of China.

Appendix A. Supplementary data

Supplementary data to this article can be found online at https://doi.org/10.1016/j.ygcen.2019.03.011.

References

Asai, M., Ramachandrappa, S., Joachim, M., Shen, Y., Zhang, R., Nuthalapati, N., Ramanathan, V., Strochlic, D.E., Ferket, P., Linhart, K., Ho, C., Novoselova, T.V., Garg, S., Ridderstrale, M., Marcus, C., Hirschhorn, J.N., Keogh, J.M., O'Rahilly, S., Chan, L.F., Clark, A.J., Farooqi, I.S., Majzoub, J.A., 2013. Loss of function of the melanocortin 2 receptor accessory protein 2 is associated with mammalian obesity. Science 341, 275–278.

Aspiras, A.C., Rohner, N., Martineau, B., Borowsky, R.L., Tabin, C.J., 2015. Melanocortin 4 receptor mutations contribute to the adaptation of cavefish to nutrient-poor conditions. Proc. Natl. Acad. Sci. USA 112, 9668–9673.

Balthasar, N., Dalgaard, L.T., Lee, C.E., Yu, J., Funahashi, H., Williams, T., Ferreira, M., Tang, V., McGovern, R.A., Kenny, C.D., Christiansen, L.M., Edelstein, E., Choi, B., Boss, O., Aschkenasi, C., Zhang, C.Y., Mountjoy, K., Kishi, T., Elmquist, J.K., Lowell, B.B., 2005. Divergence of melanocortin pathways in the control of food intake and energy expenditure. Cell 123, 493–505.

Begriche, K., Marston, O.J., Rossi, J., Burke, L.K., McDonald, P., Heisler, L.K., Butler, A.A., 2012. Melanocortin-3 receptors are involved in adaptation to restricted feeding. Genes Brain Behav. 11, 291–302.

Butler, A.A., Kesterson, R.A., Khong, K., Cullen, M.J., Pelleymounter, M.A., Dekoning, J., Baetscher, M., Cone, R.D., 2000. A unique metabolic syndrome causes obesity in the melanocortin-3 receptor-deficient mouse. Endocrinology 141, 3518–3521.

Chai, B., Li, J.Y., Zhang, W., Ammori, J.B., Mulholland, M.W., 2007. Melanocortin-3 receptor activates MAP kinase via PI3 kinase. Regul. Pept. 139, 115–121.

Chaly, A.L., Srisai, D., Gardner, E.E., Sebag, J.A., 2016. The Melanocortin Receptor Accessory Protein 2 promotes food intake through inhibition of the Prokineticin Receptor-1. eLife 5, e12397.

Chan, L.F., Webb, T.R., Chung, T.T., Meimaridou, E., Cooray, S.N., Guasti, L., Chapple, J.P., Egertova, M., Elphick, M.R., Cheetham, M.E., Metherell, L.A., Clark, A.J., 2009. MRAP and MRAP2 are bidirectional regulators of the melanocortin receptor family. Proc. Natl. Acad. Sci. USA 106, 6146–6151.

Chen, A.S., Marsh, D.J., Trumbauer, M.E., Frazier, E.G., Guan, X.M., Yu, H., Rosenblum, C.I., Vongs, A., Feng, Y., Cao, L., Metzger, J.M., Strack, A.M., Camacho, R.E., Mellin, T.N., Nunes, C.N., Min, W., Fisher, J., Gopal-Truter, S., MacIntyre, D.E., Chen, H.Y., Van der Ploeg, L.H., 2000. Inactivation of the mouse melanocortin-3 receptor results in increased fat mass and reduced lean body mass. Nat. Genet. 26, 97–102.

Chen, C., Okayama, H., 1987. High-efficiency transformation of mammalian cells by plasmid DNA. Mol. Cell. Biol. 7, 2745–2752.

Chen, W., Kelly, M.A., Opitz-Araya, X., Thomas, R.E., Low, M.J., Cone, R.D., 1997. Exocrine gland dysfunction in MC5-R-deficient mice: evidence for coordinated regulation of exocrine gland function by melanocortin peptides. Cell 91, 789–798.

Chung, T.T., Chan, L.F., Metherell, L.A., Clark, A.J.L., 2010. Phenotypic characteristics of familial glucocorticoid deficiency (FGD) type 1 and 2. Clin. Endocrinol. 72, 589–594.

Cone, R.D., 2006. Studies on the physiological functions of the melanocortin system. Endocr. Rev. 27, 736–749.

Daniels, D., Patten, C.S., Roth, J.D., Yee, D.K., Fluharty, S.J., 2003. Melanocortin receptor signaling through mitogen-activated protein kinase in vitro and in rat hypothalamus. Brain Res. 986, 1–11.

Demidowich, A.P., Jun, J.Y., Yanovski, J.A., 2017. Polymorphisms and mutations in the melanocortin-3 receptor and their relation to human obesity. Biochim. Biophys. Acta 1863, 2468–2476.

Fan, Z.C., Sartin, J.L., Tao, Y.X., 2008. Molecular cloning and pharmacological characterization of porcine melanocortin-3 receptor. J. Endocrinol. 196, 139–148.

Gantz, I., Konda, Y., Tashiro, T., Shimoto, Y., Miwa, H., Munzert, G., Watson, S.J., DelValle, J., Yamada, T., 1993a. Molecular cloning of a novel melanocortin receptor. J. Biol. Chem. 268, 8246–8250.

Gantz, I., Miwa, H., Konda, Y., Shimoto, Y., Tashiro, T., Watson, S.J., DelValle, J., Yamada, T., 1993b. Molecular cloning, expression, and gene localization of a fourth melanocortin receptor. J. Biol. Chem. 268, 15174–15179.

Ghamari-Langroudi, M., Cakir, I., Lippert, R.N., Sweeney, P., Litt, M.J., Ellacott, K.L.J., Cone, R.D., 2018. Regulation of energy rheostasis by the melanocortin-3 receptor. Sci. Adv. 4, eaat0866.

Girardet, C., Butler, A.A., 2014. Neural melanocortin receptors in obesity and related metabolic disorders. Biochim. Biophys. Acta 1842, 482–494.

Grieco, P., Balse, P.M., Weinberg, D., MacNeil, T., Hruby, V.J., 2000. D-Amino acid scan of γ-melanocyte-stimulating hormone: importance of Trp^8 on human MC3 receptor selectivity. J. Med. Chem. 43, 4998–5002.

Haitina, T., Klovins, J., Andersson, J., Fredriksson, R., Lagerstrom, M.C., Larhammar, D., Larson, E.T., Schioth, H.B., 2004. Cloning, tissue distribution, pharmacology and three-dimensional modelling of melanocortin receptors 4 and 5 in rainbow trout suggest close evolutionary relationship of these subtypes. Biochem. J. 380, 475–486.

He, S., Tao, Y.X., 2014. Defect in MAPK signaling as a cause for monogenic obesity caused by inactivating mutations in the melanocortin-4 receptor gene. Int. J. Biol. Sci. 10, 1128–1137.

Hinney, A., Volckmar, A.L., Knoll, N., 2013. Melanocortin-4 receptor in energy homeostasis and obesity pathogenesis. Prog. Mol. Biol. Transl. Sci. 114, 147–191.

Hirata, F., Strittmatter, W.J., Axelrod, J., 1979. β-Adrenergic receptor agonists increase phospholipid methylation, membrane fluidity, and β-adrenergic receptor-adenylate cyclase coupling. Proc. Natl. Acad. Sci. USA 76, 368–372.

Huang, H., Tao, Y.X., 2014. Functions of the DRY motif and intracellular loop 2 of human melanocortin 3 receptor. J. Mol. Endocrinol. 53, 319–330.

Huszar, D., Lynch, C.A., Fairchild-Huntress, V., Dunmore, J.H., Fang, Q., Berkemeier, L.R., Gu, W., Kesterson, R.A., Boston, B.A., Cone, R.D., Smith, F.J., Campfield, L.A., Burn, P., Lee, F., 1997. Targeted disruption of the melanocortin-4 receptor results in obesity in mice. Cell 88, 131–141.

Karsi, A., Waldbieser, G.C., Small, B.C., Liu, Z., Wolters, W.R., 2004. Molecular cloning of proopiomelanocortin cDNA and multi-tissue mRNA expression in channel catfish. Gen. Comp. Endocrinol. 137, 312–321.

Kay, E.I., Botha, R., Montgomery, J.M., Mountjoy, K.G., 2013. hMRAPa increases α MSH-induced hMC1R and hMC3R functional coupling and hMC4R constitutive activity. J. Mol. Endocrinol. 50, 203–215.

Klovins, J., Haitina, T., Fridmanis, D., Kilianova, Z., Kapa, I., Fredriksson, R., Gallo-Payet, N., Schioth, H.B., 2004a. The melanocortin system in Fugu: determination of POMC/AGRP/MCR gene repertoire and synteny, as well as pharmacology and anatomical distribution of the MCRs. Mol. Biol. Evol. 21, 563–579.

Klovins, J., Haitina, T., Ringholm, A., Lowgren, M., Fridmanis, D., Slaidina, M., Stier, S., Schioth, H.B., 2004b. Cloning of two melanocortin (MC) receptors in spiny dogfish: MC3 receptor in cartilaginous fish shows high affinity to ACTH-derived peptides while it has lower preference to γ-MSH. Eur. J. Biochem. 271, 4320–4331.

Kobayashi, Y., Tsuchiya, K., Yamanome, T., Schioth, H.B., Kawauchi, H., Takahashi, A., 2008. Food deprivation increases the expression of melanocortin-4 receptor in the liver of barfin flounder, *Verasper moseri*. Gen. Comp. Endocrinol. 155, 280–287.

Kumar, S., Stecher, G., Li, M., Knyaz, C., Tamura, K., 2018. MEGA X: molecular evolutionary genetics analysis across computing platforms. Mol. Biol. Evol. 35, 1547–1549.

Li, J.T., Yang, Z., Chen, H.P., Zhu, C.H., Deng, S.P., Li, G.L., Tao, Y.X., 2016. Molecular cloning, tissue distribution, and pharmacological characterization of melanocortin-4 receptor in spotted scat, *Scatophagus argus*. Gen. Comp. Endocrinol. 230–231, 143–152.

Li, L., Yang, Z., Zhang, Y.P., He, S., Liang, X.F., Tao, Y.X., 2017. Molecular cloning, tissue distribution, and pharmacological characterization of melanocortin-4 receptor in grass carp (*Ctenopharyngodon idella*). Domest. Anim. Endocrinol. 59, 140–151.

Liu, Z., Liu, S., Yao, J., Bao, L., Zhang, J., Li, Y., Jiang, C., Sun, L., Wang, R., Zhang, Y., Zhou, T., Zeng, Q., Fu, Q., Gao, S., Li, N., Koren, S., Jiang, Y., Zimin, A., Xu, P., Phillippy, A.M., Geng, X., Song, L., Sun, F., Li, C., Wang, X., Chen, A., Jin, Y., Yuan, Z., Yang, Y., Tan, S., Peatman, E., Lu, J., Qin, Z., Dunham, R., Li, Z., Sonstegard, T., Feng, J., Danzmann, R.G., Schroeder, S., Scheffler, B., Duke, M.V., Ballard, L., Kucuktas, H., Kaltenboeck, L., Liu, H., Armbruster, J., Xie, Y., Kirby, M.L., Tian, Y., Flanagan, M.E., Mu, W., Waldbieser, G.C., 2016. The channel catfish genome sequence provides insights into the evolution of scale formation in teleosts. Nat. Commun. 7, 11757.

Logan, D.W., Bryson-Richardson, R.J., Pagan, K.E., Taylor, M.S., Currie, P.D., Jackson, I.J., 2003. The structure and evolution of the melanocortin and MCH receptors in fish and mammals. Genomics 81, 184–191.

Metherell, L.A., Chapple, J.P., Cooray, S., David, A., Becker, C., Ruschendorf, F., Naville, D., Begeot, M., Khoo, B., Nurnberg, P., Huebner, A., Cheetham, M.E., Clark, A.J., 2005. Mutations in MRAP, encoding a new interacting partner of the ACTH receptor, cause familial glucocorticoid deficiency type 2. Nat. Genet. 37, 166–170.

Mo, X.L., Yang, R., Tao, Y.X., 2012. Functions of transmembrane domain 3 of human melanocortin-4 receptor. J. Mol. Endocrinol. 49, 221–235.

Mountjoy, K.G., Mortrud, M.T., Low, M.J., Simerly, R.B., Cone, R.D., 1994. Localization of the melanocortin-4 receptor (MC4-R) in neuroendocrine and autonomic control circuits in the brain. Mol. Endocrinol. 8, 1298–1308.

Mountjoy, K.G., Robbins, L.S., Mortrud, M.T., Cone, R.D., 1992. The cloning of a family of genes that encode the melanocortin receptors. Science 257, 1248–1251.

Novoselova, T.V., Larder, R., Rimmington, D., Lelliott, C., Wynn, E.H., Gorrigan, R.J., Tate, P.H., Guasti, L., O'Rahilly, S., Clark, A.J.L., 2016. Loss of *Mrap2* is associated with *Sim1* deficiency and increased circulating cholesterol. J. Endocrinol. 230, 13–26.

Palczewski, K., Kumasaka, T., Hori, T., Behnke, C.A., Motoshima, H., Fox, B.A., Le Trong, I., Teller, D.C., Okada, T., Stenkamp, R.E., Yamamoto, M., Miyano, M., 2000. Crystal structure of rhodopsin: a G protein-coupled receptor. Science 289, 739–745.

Patel, H.B., Montero-Melendez, T., Greco, K.V., Perretti, M., 2011. Melanocortin receptors as novel effectors of macrophage responses in inflammation. Front. Immunol. 2, 41.

Peterson, B.C., Waldbieser, G.C., Riley Jr, L.G., Upton, K.R., Kobayashi, Y., Small, B.C., 2012. Pre-α and postprandial changes in orexigenic and anorexigenic factors in channel catfish (*Ictalurus punctatus*). Gen. Comp. Endocrinol. 176, 231–239.

Renquist, B.J., Zhang, C., Williams, S.Y., Cone, R.D., 2013. Development of an assay for

high-throughput energy expenditure monitoring in the zebrafish. Zebrafish 10, 343–352.
Roselli-Rehfuss, L., Mountjoy, K.G., Robbins, L.S., Mortrud, M.T., Low, M.J., Tatro, J.B., Entwistle, M.L., Simerly, R.B., Cone, R.D., 1993. Identification of a receptor for γ melanotropin and other proopiomelanocortin peptides in the hypothalamus and limbic system. Proc. Natl. Acad. Sci. USA 90, 8856–8860.
Rouault, A.A.J., Srinivasan, D.K., Yin, T.C., Lee, A.A., Sebag, J.A., 2017. Melanocortin receptor accessory proteins (MRAPs): functions in the melanocortin system and beyond. Biochim. Biophys. Acta 1864, 2322–2329.
Saitou, N., Nei, M., 1987. The neighbor-joining method: a new method for reconstructing phylogenetic trees. Mol. Biol. Evol. 4, 406–425.
Sanchez, E., Rubio, V.C., Thompson, D., Metz, J., Flik, G., Millhauser, G.L., Cerda-Reverter, J.M., 2009. Phosphodiesterase inhibitor-dependent inverse agonism of agouti-related protein on melanocortin 4 receptor in sea bass (*Dicentrarchus labrax*). Am. J. Physiol. Regul. Integr. Comp. Physiol. 296, R1293–R1306.
Schonnop, L., Kleinau, G., Herrfurth, N., Volckmar, A.L., Cetindag, C., Müller, A., Peters, T., Herpertz, S., Antel, J., Hebebrand, J., 2016. Decreased melanocortin-4 receptor function conferred by an infrequent variant at the human melanocortin receptor accessory protein 2 gene. Obesity 24, 1976–1982.
Schroeter, J.C., Fenn, C.M., Small, B.C., 2015. Elucidating the roles of gut neuropeptides on channel catfish feed intake, glycemia, and hypothalamic NPY and POMC expression. Comp. Biochem. Physiol. A Mol. Integr. Physiol. 188, 168–174.
Sebag, J.A., Zhang, C., Hinkle, P.M., Bradshaw, A.M., Cone, R.D., 2013. Developmental control of the melanocortin-4 receptor by MRAP2 proteins in zebrafish. Science 341, 278–281.
Selz, Y., Braasch, I., Hoffmann, C., Schmidt, C., Schultheis, C., Schartl, M., Volff, J.N., 2007. Evolution of melanocortin receptors in teleost fish: the melanocortin type 1 receptor. Gene 401, 114–122.
Srisai, D., Yin, T.C., Lee, A.A., Rouault, A.A.J., Pearson, N.A., Grobe, J.L., Sebag, J.A., 2017. MRAP2 regulates ghrelin receptor signaling and hunger sensing. Nat. Commun. 8, 713.
Steiner, A.L., Kipnis, D.M., Utiger, R., Parker, C., 1969. Radioimmunoassay for the measurement of adenosine 3',5'-cyclic phosphate. Proc. Natl. Acad. Sci. USA 64, 367–373.
Sutton, G.M., Begriche, K., Kumar, K.G., Gimble, J.M., Perez-Tilve, D., Nogueiras, R., McMillan, R.P., Hulver, M.W., Tschop, M.H., Butler, A.A., 2010. Central nervous system melanocortin-3 receptors are required for synchronizing metabolism during entrainment to restricted feeding during the light cycle. FASEB J. 24, 862–872.
Sutton, G.M., Duos, B., Patterson, L.M., Berthoud, H.R., 2005. Melanocortinergic modulation of cholecystokinin-induced suppression of feeding through extracellular signal-regulated kinase signaling in rat solitary nucleus. Endocrinology 146, 3739–3747.
Sutton, G.M., Trevaskis, J.L., Hulver, M.W., McMillan, R.P., Markward, N.J., Babin, M.J., Meyer, E.A., Butler, A.A., 2006. Diet-genotype interactions in the development of the obese, insulin-resistant phenotype of C57BL/6J mice lacking melanocortin-3 or -4 receptors. Endocrinology 147, 2183–2196.
Takahashi, A., Davis, P., Reinick, C., Mizusawa, K., Sakamoto, T., Dores, R.M., 2016. Characterization of melanocortin receptors from stingray *Dasyatis akajei*, a cartilaginous fish. Gen. Comp. Endocrinol. 232, 115–124.
Tao, Y.X., 2007. Functional characterization of novel melanocortin-3 receptor mutations identified from obese subjects. Biochim. Biophys. Acta 1772, 1167–1174.
Tao, Y.X., 2009. Mutations in melanocortin-4 receptor and human obesity. Prog. Mol. Biol. Transl. Sci. 88, 173–204.
Tao, Y.X., 2010a. The melanocortin-4 receptor: physiology, pharmacology, and pathophysiology. Endocr. Rev. 31, 506–543.
Tao, Y.X., 2010b. Mutations in the melanocortin-3 receptor (MC3R) gene: impact on human obesity or adiposity. Curr. Opin. Investig. Drugs 11, 1092–1096.
Tao, Y.X., 2017. Melanocortin receptors. Biochim. Biophys. Acta 1863, 2411–2413.
Tao, Y.X., Huang, H., Wang, Z.Q., Yang, F., Williams, J.N., Nikiforovich, G.V., 2010. Constitutive activity of neural melanocortin receptors. Methods Enzymol. 484, 267–279.
Tao, Y.X., Segaloff, D.L., 2003. Functional characterization of melanocortin-4 receptor mutations associated with childhood obesity. Endocrinology 144, 4544–4551.
Tao, Y.X., Segaloff, D.L., 2004. Functional characterization of melanocortin-3 receptor variants identify a loss-of-function mutation involving an amino acid critical for G protein-coupled receptor activation. J. Clin. Endocrinol. Metab. 89, 3936–3942.
Valverde, P., Healy, E., Jackson, I., Rees, J.L., Thody, A.J., 1995. Variants of the melanocyte-stimulating hormone receptor gene are associated with red hair and fair skin in humans. Nat. Genet. 11, 328–330.
Volkoff, H., 2016. The neuroendocrine regulation of food intake in fish: a review of current knowledge. Front. Neurosci. 10, 540.
Yang, F., Huang, H., Tao, Y.X., 2015a. Biased signaling in naturally occurring mutations in human melanocortin-3 receptor gene. Int. J. Biol. Sci. 11, 423–433.
Yang, Z., Huang, Z.L., Tao, Y.X., 2015b. Functions of DPLIY motif and helix 8 of human melanocortin-3 receptor. J. Mol. Endocrinol. 55, 107–117.
Yang, Z., Tao, Y.X., 2016a. Biased signaling initiated by agouti-related peptide through human melanocortin-3 and -4 receptors. Biochim. Biophys. Acta 1862, 1485–1494.
Yang, Z., Tao, Y.X., 2016b. Mutations in melanocortin-3 receptor gene and human obesity. Prog. Mol. Biol. Transl. Sci. 140, 97–129.
Yi, T.L., Yang, L.K., Ruan, G.L., Yang, D.Q., Tao, Y.X., 2018. Melanocortin-4 receptor in swamp eel (*Monopterus albus*): cloning, tissue distribution, and pharmacology. Gene 678, 79–89.
Zhang, H.J., Xie, H.J., Wang, W., Wang, Z.Q., Tao, Y.X., 2019. Pharmacology of the giant panda (*Ailuropoda melanoleuca*) melanocortin-3 receptor. Gen. Comp. Endocrinol. https://doi.org/10.1016/j.ygcen.2018.1010.1024.
Zhang, J., Li, X., Zhou, Y., Cui, L., Li, J., Wu, C., Wan, Y., Li, J., Wang, Y., 2017. The interaction of MC3R and MC4R with MRAP2, ACTH, α-MSH and AgRP in chickens. J. Endocrinol. 234, 155–174.
Zhang, Y., Kilroy, G.E., Henagan, T.M., Prpic-Uhing, V., Richards, W.G., Bannon, A.W., Mynatt, R.L., Gettys, T.W., 2005. Targeted deletion of melanocortin receptor subtypes 3 and 4, but not CART, alters nutrient partitioning and compromises behavioral and metabolic responses to leptin. FASEB J. 19, 1482–1491.